

gr-qc/9806123

Spacetime Embedding Diagrams for Black Holes*

Donald Marolf

Physics Department, Syracuse University, Syracuse, New York 13244
(June, 1998)

Abstract

We show that the 1+1 dimensional reduction (i.e., the radial plane) of the Kruskal black hole can be embedded in 2+1 Minkowski spacetime and discuss how features of this spacetime can be seen from the embedding diagram. The purpose of this work is educational: The associated embedding diagrams may be useful for explaining aspects of black holes to students who are familiar with special relativity, but not general relativity.

COMMENT: To be submitted to the American Journal of Physics. Experts will wish only to skim appendix A and to look at the pictures.

Typeset using REVTEX

*e-mail:marolf@suhep.phy.syr.edu

I. INTRODUCTION

The diagram below appears in many popular treatments of black holes in books, magazines, and science museums.

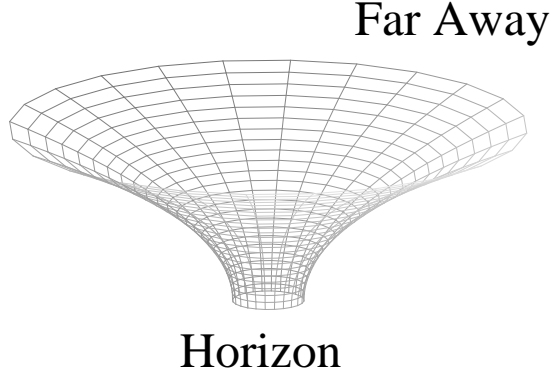


Fig. 1: The exterior $t = \text{const}$ equatorial plane of a Schwarzschild Black Hole.

It accurately represents a certain aspect of a Schwarzschild black hole, namely the intrinsic geometry of a two dimensional surface in the space around the black hole. The particular surface involved is the equatorial plane at some (Killing) time [1]. That is to say that the analogous diagram for the earth would describe the geometry of the plane indicated in fig. 2 below. Fig. 1 shows how the equatorial plane of a black hole would be curved if, instead of lying in the black hole spacetime, it were part of familiar flat Euclidean three space. Mathematically, this picture is said to represent an *embedding* of this plane into three dimensional Euclidean space.

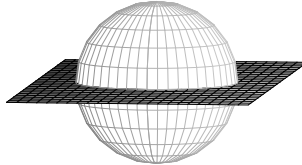


Fig. 2: The equatorial plane of the Earth.

Diagrams such as fig. 1 can be useful for explaining certain geometrical features, such as the fact that circles drawn around the equator of the black hole barely change in size as they are pushed inward or outward near the horizon. However, since they refer only to space at a single instant of time, such diagrams do not describe the most important parts of black hole physics having to do with the *spacetime* structure of the geometry.

In addition, such pictures can be misleading for the uninitiated. For example, since the bottom of the funnel in fig. 1 is the black hole horizon, students may be tempted to believe that the horizon represents a real boundary of the spacetime. Another problem is that many students believe they can see the gravitational attraction of the black hole in fig. 1 by visualizing the path of a ball ‘tossed onto the funnel.’ Technically speaking however, there is no direct connection between fig. 1 and the attraction of a black hole: there are spacetimes with the same exact spatial geometry as a black hole in which freely falling objects maintain a constant position (with respect to static worldlines), and even such spacetimes in which

objects fall in the wrong direction¹!

The purpose of the present work is to fill in this gap by creating diagrams which do show the spacetime structure of the black hole and which can therefore be used to explain this structure to students. These new diagrams will make it clear that the horizon is in fact much like any other part of the spacetime. They will also allow one to see the real gravitational ‘attraction’ of the black hole.

Specifically, the aim is to provide a means to take students familiar only with special relativity and *show* them a number of features of black holes. This work itself is presented at a slightly higher level and is intended for readers with some familiarity with the basic concepts of General Relativity and black holes, though the technical material is relegated to the appendices. A reading of, for example, one of [2–4] should provide adequate preparation, and even the reader familiar only with special relativity should be able to gain some understanding from sections III and IV.

To make our new kind of diagram, we will again choose a two dimensional surface and embed this surface in a three dimensional space. However, since we wish to show the *spacetime* aspects of the geometry, our new surface will include both a spacelike direction and a timelike direction. That is, some pairs of events on our surface will be separated by a timelike interval while other pairs will be separated by a spacelike interval. We therefore need to draw the surface inside three dimensional (2+1) Minkowski space as opposed to Euclidean three space. This means that our diagrams are most useful for students with a strong grasp of special relativity.

Technically, we will work with what is known as the Kruskal spacetime (also known as the analytically extended Schwarzschild spacetime) [5]. This describes an ‘eternal’ black hole which does not form by the collapse of matter but instead has been there forever. In particular, it describes a spherically symmetric such black hole with no electric charge or angular momentum.

The surface we consider here is the radial, or rt , plane given by $\theta = \text{const}$, $\varphi = \text{const}$ in a spherical coordinate system. Due to the spherical symmetry, it contains the worldline of any observer with zero angular momentum, whether falling freely or accelerating in a rocketship. This is also true for (fictitious) observers traveling faster than light. The radial plane is often (e.g. [6,7]) called the dimensional reduction of the 3+1 black hole to 1+1 dimensions as it is effectively a 1+1 version of a black hole².

A light review of the Kruskal spacetime is presented in section II below. The interested reader should consult [5,9] for a more thorough discussion. The embedding diagram is

¹For example, in the metric $ds^2 = -dt^2 + \frac{dr^2}{(1-2M/r)} + r^2 d\theta^2 + r^2 \sin^2 \theta d\varphi^2$, worldlines with constant r, θ, φ are freely falling. In the spacetime $ds^2 = -\frac{dt^2}{(1-2M/r)} + \frac{dr^2}{(1-2M/r)} + r^2 d\theta^2 + r^2 \sin^2 \theta d\varphi^2$, free fallers that begin at rest with respect to this coordinate system fall toward large r .

²Note, however, that it is slightly different from the 1+1 dilaton black holes of, for example, [7,8].

shown in section III, and we discuss there how it may be used to illustrate a number of general features of the black hole geometry. We save those features associated with the horizon or with the Schwarzschild coordinate system for section IV. Because of its more technical nature, the derivation of the equations describing the embedding has been placed in appendix A. Section V contains a short discussion of the results and some extensions. Finally, appendix B comments briefly on the embedding of other surfaces: the radial plane of spacetimes describing star-like objects and the analogue of fig. 1 *inside* the black hole.

II. A BRIEF REVIEW OF THE KRUSKAL SPACETIME

As stated above, the Kruskal spacetime describes an eternal black hole which exists forever. Such black holes have much in common with the usual astrophysical sort that form from the collapse of matter, but they are mathematically simpler. On the other hand, they also have certain odd features which their astrophysical cousins do not share. For example, the Kruskal spacetime contains not just one, but two separate ‘asymptotic regions’ on opposite sides of the black hole, connected by an Einstein-Rosen bridge [1]. Thus, the old kind of embedding diagram (the analogue of fig. 1) for this case involves two copies of fig. 1 glued together at the horizon as shown in fig. 3. The left and right parts are often described as two separate Universes connected by the ‘wormhole’ (Einstein-Rosen bridge) in the middle. In contrast, an astrophysical black hole has only one exterior region. As a result, only a part of the Kruskal spacetime (containing, say, the right, but not the left side of fig. 3) would be relevant to a discussion of such black holes. More will be said about this below.

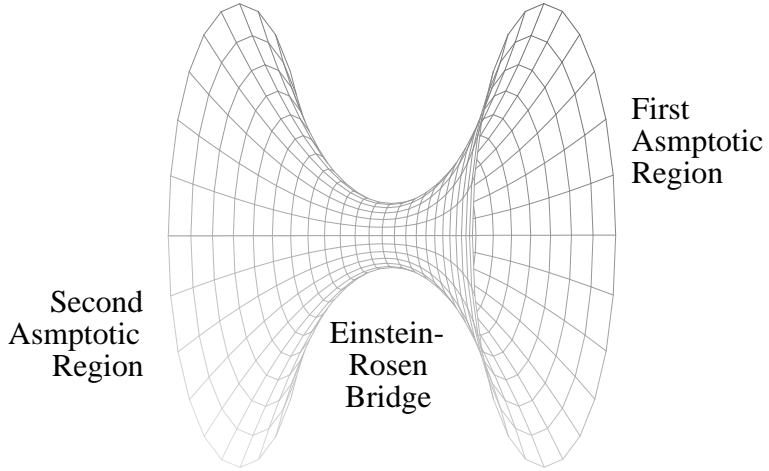


Fig. 3: The $t = \text{const}$ equatorial plane of a Kruskal black hole.

In fig. 3, we have rotated both the left and right parts of the diagram with respect to fig. 1. This serves to illustrate the fact that the orientation of these diagrams in space carries no information. It will also allow the reader to more easily relate fig. 3 to the diagrams that appear below, which are of a different sort for which the orientation in space does carry information.

We remind the reader that the global structure of the Kruskal spacetime is summarized [10] by the Penrose diagram in fig. 4. This diagram shows only the time and radial directions and does not include the angular directions around the black hole. In particular, time runs up and down and space runs left to right. This means that, figs. 3 and 4 have only one direction in common: the spatial direction which runs more or less right to left on both diagrams.

Recall that a Penrose diagram does not accurately portray distances and times, but it *is* drawn so that light rays always travel along lines at 45 degrees to the vertical, no matter how the spacetime is curved. This is a very useful property that in fact all of our remaining diagrams will share. Note that the solid lines in fig. 4 all correspond to the paths of light rays.

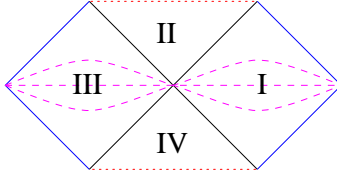


Fig. 4: The Penrose diagram for a Kruskal black hole.

Regions I and III of fig. 4 are two disconnected ‘exterior’ regions. Each dashed line shows the location of a surface like the one shown in fig. 3. The Kruskal spacetime contains infinitely many such surfaces, all exactly alike and each lying half in region I and half in region III with the ‘throat’ just at the point where the two regions touch. As mentioned above, only one of these external regions (say, I) has an analogue in astrophysical black holes.

The other regions are referred to as the interior of the black hole: region II is the ‘future interior’ and region IV is the ‘past interior.’ Since light rays travel at 45 degrees to the vertical, objects traveling at less than the speed of light can neither enter region IV nor leave region II. As a result, the light rays that form the boundaries of these regions are the horizons of the black hole. There are also two singularities, one in the past in region IV and one in the future in region II, indicated by the dotted lines on the diagram. Note that the singularities are *spacelike* lines.

The past interior (region IV) is another part of our spacetime with no analogue in an astrophysical black hole. The diagram below should clarify the relationship between such black holes and the Kruskal spacetime:

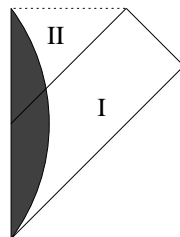


Fig. 5: The Penrose diagram for a black hole that forms from stellar collapse.

The unshaded parts of regions I and II are essentially the same as regions I and II in the Kruskal black hole. The shaded region is the star that collapses to form the black hole.

Inside the star, the spacetime is slightly different from Kruskal, though except for removing regions III and IV it is still qualitatively very similar.

We now turn to a description of the Schwarzschild coordinate system, which is a useful way to label events in the Kruskal spacetime. Briefly, this system consists of four functions, r , t , θ , and φ . The last two of these are the usual coordinates on spheres ‘around’ the black hole, with θ being a longitude-like coordinate taking values in $[0, \pi]$ and φ a latitude coordinate taking values in $[0, 2\pi]$. On the other hand, r and t are coordinates that are constant on such spheres and whose values pick out which particular sphere one is referring to. The function r tells how *big* the particular sphere is; the area of the sphere is $4\pi r^2$. An important subtlety is that r does not directly give the distance away from *anything*. In addition, the Kruskal spacetime does not have a ‘center’ at $r = 0$ in the usual sense. The last function, t , is related to a symmetry of the Kruskal spacetime. Its most important property is that, in the exterior (regions I and III), surfaces of constant t are surfaces of simultaneity for observers who do not move with respect to the black hole.

The Schwarzschild coordinate system cannot really be used on the entire Kruskal spacetime as it breaks down at the horizon. However, it can be used *separately* in the interiors of regions I, II, III, and IV. When this is done, one of the unusual features of this coordinate system is that t is only a timelike coordinate in the exterior (regions I and III). In the interior (regions II and IV), it is spacelike. Similarly, the coordinate r is spacelike in the exterior (regions I and III) where it takes values $r > 2MG/c^2$. Here, M denotes the mass of the black hole, G is Newton’s universal constant of gravitation, and c is the speed of light. In the interior (regions II and IV), r is timelike and takes values $r < 2MG/c^2$. On the horizon itself, r is a lightlike coordinate and takes the constant value $r = 2MG/c^2$. Lines of constant r and t are shown in fig. 6 below in all four regions:

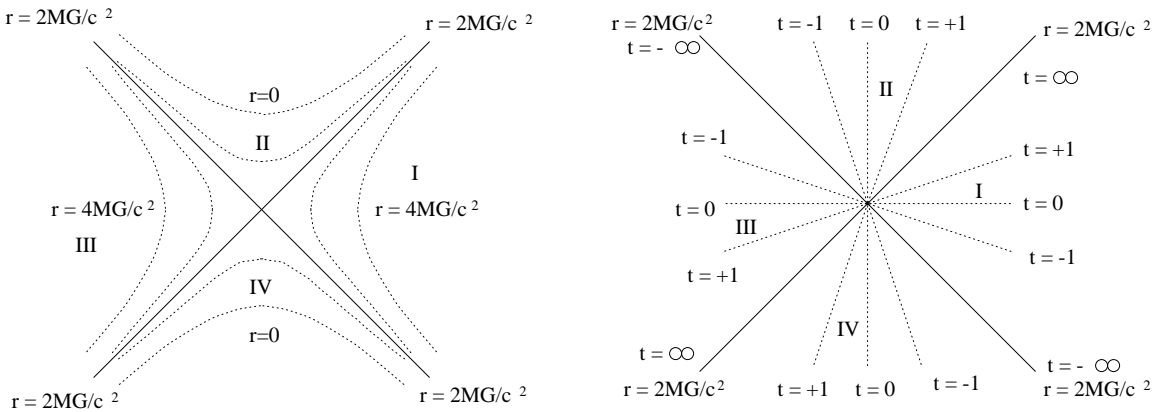


Fig. 6: The Schwarzschild coordinate system.

Again, these diagrams are drawn so that, despite the curvature of the spacetime, light rays always travel at 45 degrees to the vertical. Note that the fact that the $t = 0$ line runs through the point where the horizons cross does not make it a ‘special’ time in any way since all of the other $t = \text{const}$ lines run through this point as well. In fact, any transformation $t \rightarrow t + \text{constant}$ is a symmetry of the black hole. In the diagrams of fig. 6, this symmetry looks like a boost transformation around the origin.

As a more technical reminder, we mention that the actual geometry of the Kruskal spacetime is encoded in the metric which, in Schwarzschild coordinates, takes the form [11]

$$ds^2 = -c^2 \left(1 - 2MG/rc^2\right) dt^2 + \frac{dr^2}{1 - 2MG/rc^2} + r^2 d\theta^2 + r^2 \sin^2 \theta d\varphi^2. \quad (2.1)$$

This form holds in the interior of every region (I, II, III, and IV) but cannot be used directly at the horizons (where $r = 2MG/c^2$).

III. THE EMBEDDING DIAGRAM

The diagram below shows the embedding derived in appendix A. It illustrates what the radial (i.e., $\theta = \text{const}$, $\varphi = \text{const}$) plane of a Kruskal black hole would look like if it were a surface in 2+1 Minkowski space. As with the Penrose diagram of fig. 4, it describes only the time and radial directions, and not the angular directions.

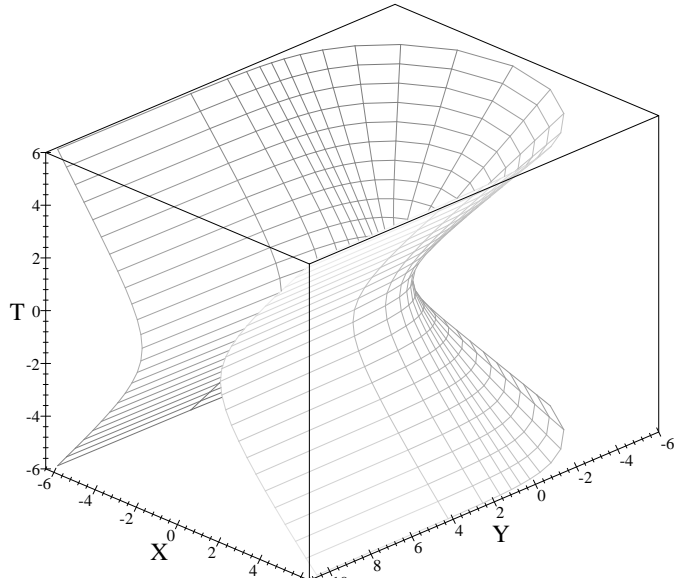


Fig. 7: The $\theta = \varphi = \text{const}$ embedding diagram for a Kruskal black hole, in units where $c = 1$ and $2MG/c^2 = 1$.

Here, the vertical (T) direction is timelike and the horizontal (X and Y) directions are spacelike. Thus, time again runs up and down while space runs across the diagram. Units have been chosen in which the speed of light (c) is one, so that light rays travel at 45 degrees to the T axis. In addition, the size of the black hole has been fixed by using units in which the ‘Schwarzschild radius’ of the horizon ($2MG/c^2$) has been set to one. The lines in fig. 7 serve only to guide the eye and do not represent any particular structure of the black hole solution.

Note that the diagram is a smooth surface, with little to distinguish one point from another. In particular, it is not immediately clear which points lie on the horizon $r = 2MG/c^2$. This is an excellent way to show students that the horizon is not essentially different from any other part of the spacetime.

As the reader may wish to view and manipulate this surface for herself, we mention that this picture was drawn with a four line Maple code. The basic idea of the code is to introduce a (not quite smooth) coordinate s on the embedded surface so that s, T each range over the real line and so that they change rapidly where the surface is flat, but slowly where the surface is highly curved. The particular code used was:

```

> X := (s,T) -> tanh(5*s/2)*sqrt(s^2 + T^2);
> sigma := (s,t) -> (X(s,T))^2 - T^2 ;
> Y := (s,T) -> evalf( int( sqrt( ( (1-q)^(-4) - 1 ) /q ), q=0..sigma(s,T)/4),2);
> plot3d([Y(s,T),X(s,T),T],s = -1.8 ..1.8, T = -5..5, scaling=constrained,
axes=box, labels=[Y,X,T], orientation=[45,65], axesfont=[TIMES,ROMAN,14],
labelfont=[TIMES, ROMAN, 18]);

```

The integration variable q corresponds to $\sigma/16M^2$ from appendix A.

Let us now examine the basic features of our diagram. Note that it has two long ‘flanges’ (marked below in fig. 8) which project out in the positive Y direction.

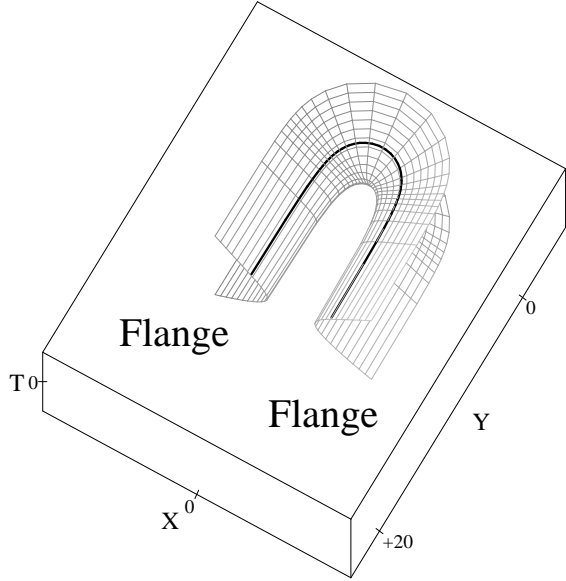


Fig. 8: The asymptotic regions.

Moving along the flanges in the $+Y$ direction (say, along the heavy line in fig. 8 above) allows one to move a large proper distance in a spacelike direction. Thus, these flanges must correspond to the asymptotic regions far away from the black hole. This is also clear from equation (A5) in appendix A. We may, for example, take the right flange to represent region I of the Penrose diagram (fig. 4) and the left flange to represent region III.

Now, far from the black hole (that is, far out on these flanges), spacetime should be flat. We can see that this is so from the above pictures. If we move far enough out along a given flange, the black line in fig. 8 becomes straight. Thus, the flanges are curved only in the XT plane and not in the YT or XY planes. A surface that is curved only in one direction (when embedded in a flat three space) has zero intrinsic curvature, e.g., a cylinder is flat. In this way, we can see that the intrinsic curvature of our slice vanishes as we move away

from the black hole.

One of the most important uses of this sort of diagram is that it does allow one to see the gravitational ‘attraction’ of the black hole. Specifically, it allows one to see the worldlines followed by freely falling observers, and to see that they curve toward the middle of the diagram, away from the asymptotic regions. The point is that, in General Relativity, freely falling observers follow ‘geodesics,’ the straightest possible lines on a curved surface. Human beings are in fact quite good at visualizing such lines, just by pretending that they are ‘walking’ up the surface shown in the embedding diagram³ (fig. 7). For example, visualizing a person walking around a sphere shows that geodesics on a sphere are just the great circles⁴

Thus, let us consider a freely falling observer moving up one of the flanges. Because our surface bends *away* from the ends of the flanges and *toward* the center, our observer will follow this curve and also move closer to the center of the surface. A computer generated geodesic of this type is shown in fig. 9 below.

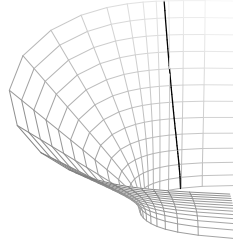
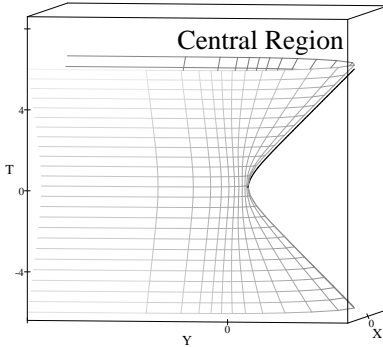


Fig. 9: The worldline of an observer who falls freely from rest at $r = 3MG/c^2$, starting at $T=0$.

Between the two asymptotic regions, the surface is curved. Note that the central portion of the surface rapidly approaches a light cone:



³An observer must walk more or less ‘up’ the diagram, as we assume that the motion is forward in time and at less than light speed.

⁴The present case is slightly different as we deal with a curved surface in Minkowski space and not in Euclidean space. This will lead the human eye to make some errors, but they are typically small.

Fig. 10: The central portion rapidly approaches a light cone.

It turns out that this is what accounts for the fact that we see no direct visual sign of the black hole singularity. Equation (A6) from appendix A shows that the singularity $r = 0$ is in fact located at $T = \pm\infty$ in the distant future and past. The point here is that our surface approaches a light cone (along which no proper time would pass) so quickly that, if we follow a line up the center of this diagram (such as the black line at the right edge of fig. 10 above), it reaches $T = \pm\infty$ after only a finite proper time. Thus, although the black hole singularity lies at the boundary of the spacetime, an observer will reach it in a finite proper time. A nice feature of the diagram is that it shows that the singularity does not occur at any *place* inside the black hole. Instead, it is better thought of as occurring at some *time*, which in this case happens to be $T = \pm\infty$.

Now, a tricky point of the diagram is that, despite the fact that $r = 0$ is a curvature singularity, the surface appears to become flat as we follow it toward the singularity at $T = \pm\infty$. This is a result of the fact that the surface is drawn from a fixed reference frame in the 2+1 Minkowski space while observers traveling in the surface are (for large T) moving at nearly the speed of light with respect to that frame. For example, the worldline in fig. 11 is moving much faster (relative to the frame in which the diagram is drawn) at event E5 than at event E1. In fact, each successive event drawn corresponds to an increase of the boost parameter ($\tanh^{-1}(v/c)$) by 0.5.

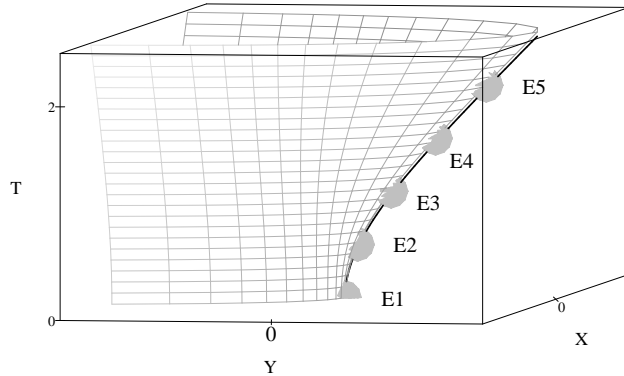


Fig. 11: Five events along a freely falling worldline.

The familiar effects of time dilation and length contraction have the effect of ‘flattening out’ the diagram. The fact that a finite bit of proper time is expanded to reach all the way to $T = \pm\infty$ means that, for large T , we are given such a close up view of the surface that the curvature is not visible. To actually *see* the curvature at some event with our eyes, we must redraw the picture in a set of reference frames in which an observer at that event is at rest. Thus, we must consider a series of more and more highly boosted reference frames. Below, we have used a series of boosts in the YT plane to redraw the embedding diagram in the reference frame of the wordline from fig. 11 at each of the events E1, E2, E3, E4, and E5.

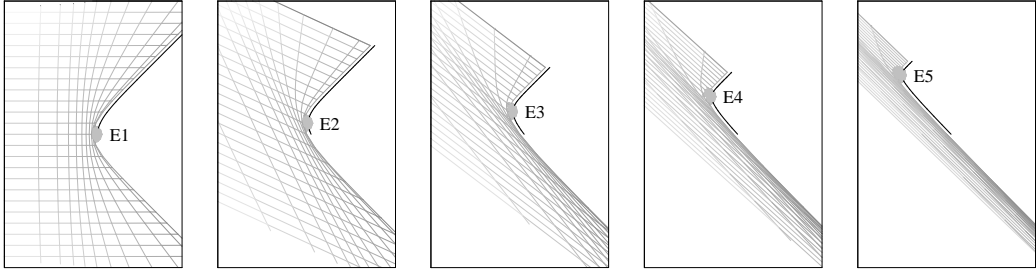


Fig. 12: The embedding diagram viewed from the side and boosted into the reference frame of the indicated worldline at E1, E2, E3, E4, and E5.

The singularity is now evident in the fact that, as we increase the boost and so examine points closer and closer to its location, the ‘corner’ in the diagram becomes sharper and sharper. This shows that the intrinsic curvature of the surface becomes larger and larger as T increases and r goes to zero. Physically, we can see that geodesics which are close to each other before the corner diverge much more quickly after passing E5 than after passing E1. The diagrams in fig. 13 below each show the same two geodesics, but from the reference frames of E1, E2, E3, E4, and E5 respectively.

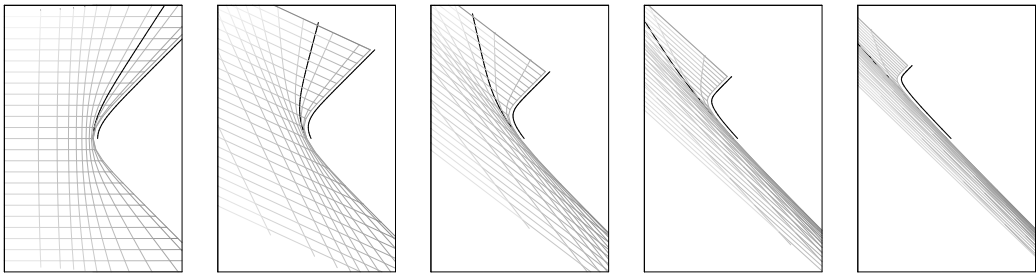


Fig. 13: The intrinsic divergence of two nearby worldlines near different events.

IV. THE HORIZON AND SCHWARZSCHILD COORDINATES

It is instructive to discover the horizons of the black hole by directly examining the embedding diagram without making reference to the equations in appendix A. Recall that the future horizons are the edges of the region (II) from which an observer cannot escape without traveling faster than light. Similarly, the past horizons are the boundaries of the region (IV) that an observer (starting far away) cannot enter without traveling faster than light.

Note that the two light rays given by $Y = 0$, $X = \pm T$ (shown in fig. 14) lie completely in our surface. The reader will immediately see that these light rays do not move along the flanges at all (since they stay at $Y = 0$) and thus neither of these light rays actually move away from the black hole. Instead, the light rays are trapped near the black hole forever. It is also clear that these light rays divide our surface into four regions (I, II, III, and IV) much as in figs. 4 and 6. Thus, an observer in region II of our spacetime cannot cross one of these light rays without traveling faster than the speed of light. Observers in this region are trapped inside the black hole.

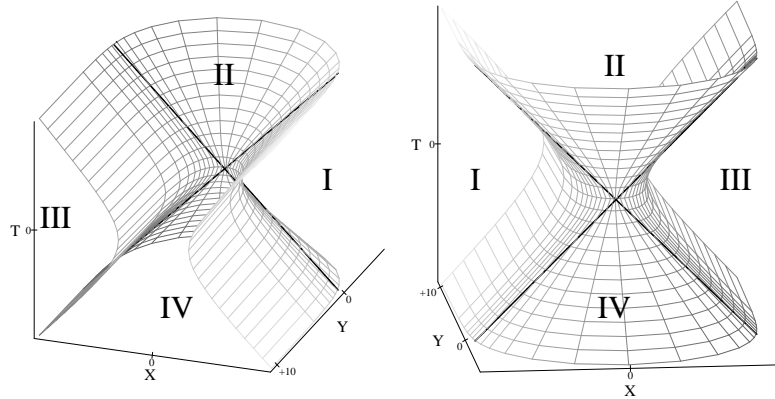


Fig. 14: The lines $Y = 0$, $X = \pm T$ divide the diagram into four regions.

On the other hand, any light ray fired outward from region I or III of our surface *will* eventually reach large values of Y and thus escape from the black hole. Thus, the light rays at $Y = 0$, $X = \pm T$ (for $T > 0$) are the future horizons of the black hole. Similarly, these same light rays for $T < 0$ form the past horizons of the black hole. This may also be seen from equations (A5) and (A6) in appendix A.

We now turn again to the Schwarzschild coordinates r and t which were briefly reviewed in section II. Insight into this coordinate system can be gained by drawing these coordinates directly on our embedding diagram:

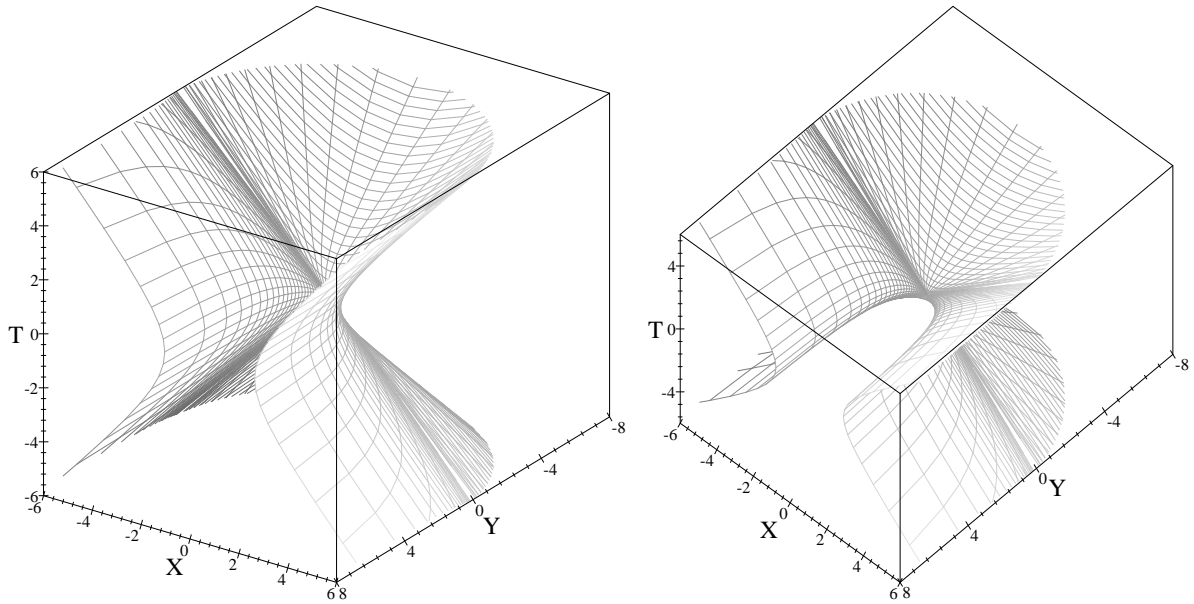


Fig. 15: Two views of the embedding diagram with Schwarzschild coordinate lines.

This has also been done with a short Maple code. In this case, it is easiest to first have Maple draw each region (I,II,III,IV) separately, as we can then use r, t as intrinsic coordinates in the surface and Maple's plotting algorithm will draw the lines of constant r, t for us. The four pieces can then be combined into a single diagram. Thus, region I can be drawn using the code:

```
> X1 := (s,f) -> s*cosh(f); T1 := (s,f) -> s*sinh(f);
```

```

> Y1 := (s,f) -> evalf(int( sqrt(( (1-q)^( -4) -1)/q),q=0..(s^ 2)/4),2);
> bh1:=plot3d([Y1(s,f),X1(s,f),T1(s,f)], s=0..1.84, f=-3..3, scaling=constrained,
  axes=box, labels=[Y,X,T],axesfont=[TIMES,ROMAN,14],
  labelfont=[TIMES,ROMAN, 18]); bh1;

```

For those who have read appendix A, we mention that f is the hyperbolic angle ϕ and s is proportional to the proper distance ρ , which is a function of r . In this way, lines of constant s or f are constant r and t lines respectively⁵. Again, the integration variable q corresponds to $\sigma/16M^2$ and the diagram is shown in units where $2MG/c^2 = 1$; thus, $s^2 = \sigma/4M^2$.

Region II is drawn with the code:

```

> X2 := (s,f) -> s*sinh(f); T2 := (s,f) -> s*cosh(f);
> Y2 := (s,f) -> evalf(int( sqrt(( (1-q)^( -4) -1)/q),q=0..(-s^ 2)/4),2);
> bh2:=plot3d([Y2(s,f),X2(s,f),T2(s,f)],s=0..6, f=-3..3, scaling=constrained,
  axes=box, labels=[Y,X,T],axesfont=[TIMES,ROMAN,14],
  labelfont=[TIMES,ROMAN, 18]); bh2;

```

Regions III and IV can be drawn in the same way, or obtained by an appropriate rotation of regions I and II.

Recall from fig. 6 that the horizon lies at $t = \pm\infty$ in Schwarzschild coordinates. Since Maple is not be able to draw the surface all the way to $t = \pm\infty$, there is a slight gap in the diagram at the horizon which serves to illustrate its position. The horizon is also clearly marked (even in the region where no gap is visible) as a large “X” due to the fact that the lines of constant t pile up near $t = \pm\infty$.

As discussed in section II, the lines of constant t are spacelike in regions I and III (where t is a timelike coordinate) and are timelike in regions II and IV (where t is a spacelike coordinate). Thus, the lines running across the flanges (in regions I and III) are constant t as are the lines running up and down the central light cone (in regions II and IV). The black lines in fig. 16 below show the location of a few constant t lines in each region. As seen previously in fig. 6, all lines of constant t intersect at a common point, in our case at $X = Y = T = 0$.

⁵Of course, the constant r lines drawn in this way are not equally spaced contours of r . Rather, they are equally spaced contours of s . If one wishes, this is easily corrected by replacing s with $\sqrt{|1 - \frac{2M}{r}|}$. However, this makes it more difficult to see the geometry of the surface, as r changes slowly in some regions where the surface is tightly curved.

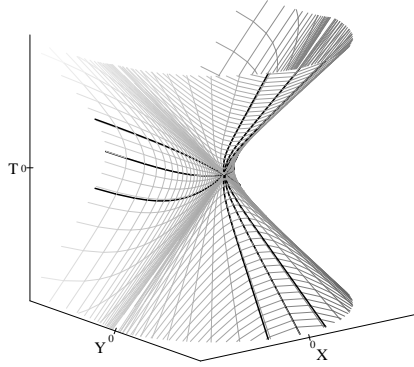


Fig. 16: Lines of constant t in each region.

On the other hand, lines of constant r run up the flanges in regions I and III and across the light cones in regions II and IV, as shown by the black lines in fig. 17. A useful property of these lines to know is that a given line of constant r lies entirely in a plane of constant Y , as is clear from the second diagram in fig. 17. In particular, as was already noted, the horizons are located at $r = 2MG/c^2$ and lie in the $Y = 0$ plane. The $Y > 0$ region has $r > 2MG/c^2$ and corresponds to outside the black hole, while the $Y < 0$ region has $r < 2MG/c^2$ and corresponds to the inside. As was already stated, $r = 0$ is the singularity and is located inside the horizons at $T = \pm\infty$. The reader will notice a strong similarity between the first diagram in fig. 17 and the symmetry transformation of fig. 8. This is because the symmetry does not r and therefore only slides events back and forth along lines of constant r .

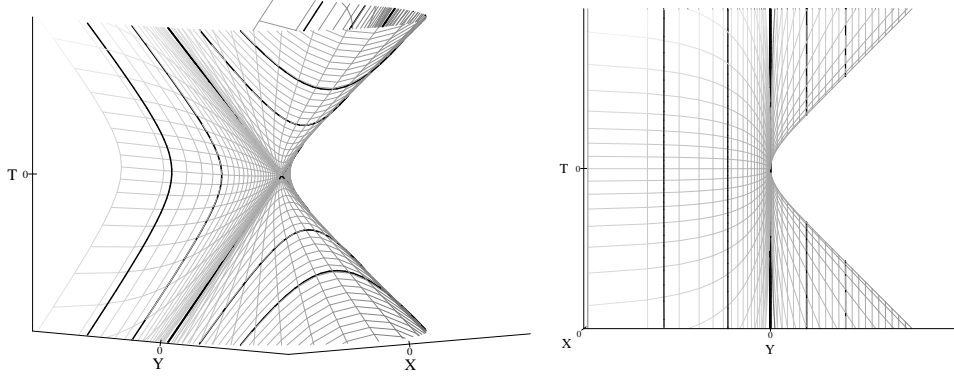


Fig. 17: The lines $r = 8MG/c^2$, $r = 4MG/c^2$, $r = 2MG/c^2$, $r = MG/c^2$, and $r = MG/2c^2$.

Such diagrams are useful for seeing the large acceleration (tightly curved worldlines) of observers who remain at constant r just outside the horizon. Here, we should perhaps pause to remind the reader which aspects of our diagram represent ‘physical’ effects and which do not. The important point here is that the ambient Minkowski space is *only* a mechanism for visualizing the surface and, by itself, carries no physical information. In particular, the way that a worldline bends relative to the ambient Minkowski space is not important by itself, so long as the entire surface is bending in the same way. What *is* important, and what does correspond to the proper acceleration of a worldline in the black hole spacetime is that way

that the worldline bends *within* our surface.

Now, the constant r lines in fig. 17 all bend only in the XT plane; they remain at a constant value of Y . This means that their proper acceleration vector (in the ambient Minkowski space at, say, $T = 0$) points in the $+X$ direction. Now, close to the middle of our diagram, the $+X$ direction is more or less tangent to our surface. Thus, the proper acceleration has a large component tangent to our surface, and these worldlines have a large proper acceleration *in* the black hole spacetime. This corresponds to the fact that a spaceship which is close to the black hole must fire its rockets with a large thrust in order not to fall in. In contrast, far away from the black hole the $+X$ direction is almost completely orthogonal to our surface at $T = 0$. Thus, the proper acceleration of such worldlines *within* our surface is virtually zero, and spaceships far enough away from the black hole need only the slightest thrust to avoid falling in.

Another useful feature of the Schwarzschild coordinates is that they illustrate the gravitational time dilation (redshift) that occurs near a black hole. Recall from section II that the $t = \text{const}$ lines are lines of simultaneity for the family of (accelerated) observers who follow worldlines of constant r). Now, note that (as shown in fig. 18 below) the spacing between the $t = \text{const}$ lines outside the black hole varies with r , so that static observers at different values of r have clocks that accumulate proper time at different rates:

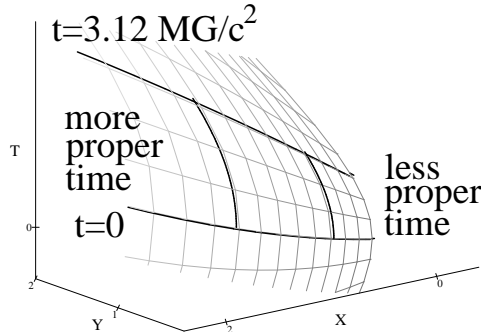


Fig. 18: Static observers experiencing more and less proper time between two constant t lines.

As a final feature, we point out that the infinite stretching of objects due to the gravitational tidal forces in the radial direction near the singularity can also be seen from fig. 15. The point here is that a line of constant t (in the interior) is a timelike geodesic. Thus, it is the worldline of some freely falling observer. Consider two such lines, one at $t = t_0$ and one at $t = t_0 + \delta$, such as the ones shown in fig. 19:

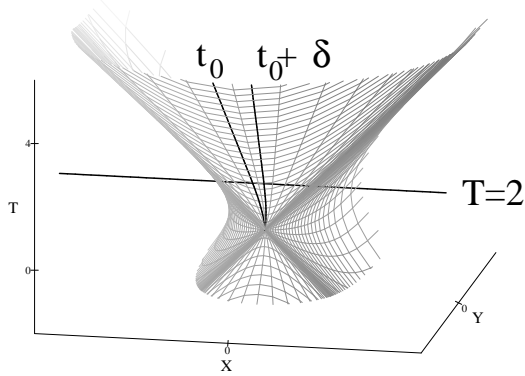


Fig. 19: Worldlines following $t = t_0$ and $t = t_0 + \delta$.

For small δ , these observers are very close to each other and are nearly at rest relative to each other at, say, $T = 2$. On the other hand, we can see that, if we wait until $T = +\infty$ (when they hit the singularity), they will be infinitely far apart (say, as measured along a line of constant r). But $T = +\infty$ is only a short *proper* time in the future! Thus, the two geodesics will separate infinitely far in a finite proper time. It follows that their relative acceleration (or, equivalently, the gravitational tidal ‘force’) diverges as $T \rightarrow \infty$.

V. DISCUSSION

We have constructed an embedding of the radial plane of the Kruskal black hole in 2+1 Minkowski space and used it to illustrate certain features of black hole spacetimes. Such diagrams may be of use in describing black holes to students familiar with special, but not general, relativity. In particular, such diagrams make it clear that the horizon is a smooth subsurface of the spacetime and show the gravitational attraction of the black hole.

Unfortunately, not all two dimensional surfaces with one spacelike and one timelike direction can be embedded in 2+1 Minkowski space. This is much the same as trying to embed two dimensional Riemannian spaces in three dimensional Euclidean space (and it is well known that, for example, the two dimensional surface of constant negative curvature cannot be so embedded). Thus, a completely general spacetime cannot be treated in the same way. However, appendix B 1 shows that it is in fact possible to embed the radial plane of any spacetime which describes a ‘normal’ static and spherically symmetric star-like object (without horizons or regions of infinite density). As an example, for a ‘star’ made of a thin spherical shell of mass M located at $r = 4MG/c^2$, the associated embedding diagram is:

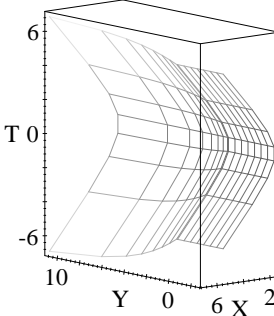


Fig. 20: The embedding diagram for a static thin shell of mass M at $r = 4MG/c^2$, shown in units with $c = 1$ and $2MG/c^2 = 1$.

The shell is located at the ‘crease’ and lines of constant Schwarzschild radius r and time t have been shown. Such diagrams may serve to give students an intuitive picture of the way that matter curves spacetime in General Relativity. In particular, it may be of interest to study such diagrams for stars with different equations of state to get a feeling for the different gravitational effects of pressure and density.

More general embeddings of black hole spacetimes with horizons should be possible as well. In particular, a study of the embedding of the radial plane of the Reissner-Nördstrom black hole is in progress.

ACKNOWLEDGMENTS

I would like to thank Alan Middleton for his assistance with Maple and Peter Saulson for helpful comments and advice. This work was supported in part by NSF grant PHY-9722362 and funds provided by Syracuse University.

APPENDIX A: EMBEDDING THE RADIAL PLANE

In this appendix, we derive the equations that describe the embedding shown in fig. 7. Recall that we consider the radial plane given by setting the angular coordinates θ, φ to (arbitrary) fixed values and letting r, t range over all of their values. The motion of any observer which maintains zero angular momentum must take place in such a plane whether the observer falls through the horizon or remains outside. Since $d\theta = 0 = d\varphi$ on this plane, the metric on our surface is given by the first two terms of (2.1):

$$ds^2 = - \left(1 - \frac{2M}{r}\right) dt^2 + \frac{dr^2}{1 - \frac{2M}{r}}. \quad (\text{A1})$$

In this equation, and in the rest of the appendix, we use units in which Newton’s constant (G) and the speed of light (c) are set equal to one.

Let us begin with region I. To construct the embedding, we will make use of the symmetries of the spacetime. This region has a time translation symmetry given by $t \rightarrow t + \Delta t$.

However, we see from the metric (2.1) that, under such a symmetry transformation, not all points on the surface are displaced through an equal amount of proper time. Instead, a point at coordinate r is displaced through a proper time $\Delta t \sqrt{1 - 2M/r}$. This is the familiar gravitational redshift near the horizon of a black hole.

Thus, in order to embed region I of our surface, we will need to find a timelike symmetry of 2+1 Minkowski space which also displaces different points through different amounts of proper time. Let us endow our 2+1 Minkowski space with Cartesian coordinates X, Y, T in the usual way. One such symmetry is a boost of the Minkowski space, say, in the X, T plane. Of course, this symmetry is not timelike everywhere on Minkowski space, but induces a division of this spacetime into four regions in a manner analogous to figs. 4 and 6. The boost is timelike in regions I and III and spacelike in regions II and IV. Since the time translation on the Kruskal spacetime has the same property, this boost is a good candidate for the analogue of a time translation in our embedding space. We expect each of the regions I,II,III,IV of the radial Kruskal plane to embed in the corresponding region of Minkowski space.

Having realized this, it is useful to introduce coordinates on Minkowski space that are adapted to the boost symmetry. In region I ($X > |T|$), let

$$\begin{aligned}\rho &= \sqrt{X^2 - T^2}, \\ \phi &= \tanh^{-1}(T/X).\end{aligned}\tag{A2}$$

These are just the usual proper distance and hyperbolic angle in region I of the X, T plane. In these coordinates, the metric on our Minkowski space is

$$ds^2 = -\rho^2 d\phi^2 + d\rho^2 + dY^2\tag{A3}$$

and a boost corresponds to $\phi \rightarrow \phi + \Delta$. Thus, ϕ should be proportional to the t of our embedded plane. We will choose to set $\phi = \frac{t}{4M}$ as this choice will lead to a smooth embedding.

It follows that a boost that sends ϕ to $\phi + \Delta$ corresponds to a time translation that sends t to $t + 4M\Delta$. This moves a point at ρ in the Minkowski space by $\rho\Delta$ and a point at r in the Kruskal spacetime by $(1 - 2M/r)^{1/2}4M\Delta$. Therefore, we must set $\rho = 4M\sqrt{1 - 2M/r}$. To complete our construction of the embedding, we need only give Y as a function of r and t . By symmetry, it can in fact depend only on r . The function $Y(r)$ is determined by the requirement that the metrics agree on a $t = 4M\phi = \text{const}$ slice:

$$\frac{dr^2}{1 - 2M/r} = ds^2 = d\rho^2 + dY^2.\tag{A4}$$

Solving this equation yields

$$Y(r) = \int_{2M}^r \sqrt{\left(1 + \frac{2M}{r} + \frac{4M^2}{r^2} + \frac{8M^3}{r^3}\right)} dr.\tag{A5}$$

Here, we have chosen the horizon $r = 2M$ to be located at $Y = 0$. It may now be checked that the induced metric on the surface $\phi = t/4M$, $\rho = 4M\sqrt{1 - 2M/r}$, $Y = Y(r)$ in region I is given by the first two terms of (2.1). Note that, for any r , $\rho^2 < 16M^2$.

This completes our embedding of region I of the radial Kruskal plane in region I of the 2+1 Minkowski space. The embedding of region III is exactly the same, except that we work in region III of the Minkowski space so that $X < 0$. In regions II and IV, we introduce ρ as the proper time from the origin in the T, X plane and ϕ as the associated hyperbolic angle $\tanh^{-1}(X/T)$. The discussion differs from that of regions I and III by an occasional sign at the intermediate steps, so that, for example, $\rho = 4M\sqrt{\frac{2M}{r} - 1}$. However, in the end we arrive at exactly the same expression (A5) for $Y(r)$. This feature depends on the precise choice of the proportionality factor between t and ϕ and justifies the choice (4M) made above.

Thus, we have smoothly embedded the four regions I,II,III,IV of the Kruskal spacetime in 2+1 Minkowski space. These four pieces in fact join together to form a single smooth surface. To verify this, we need only show that, on our surface, one of the embedding coordinates (say, Y) is a smooth function of the other two (X, T). We have written Y as a smooth function of r , so we must now study r as a function of X and T . We have written r in a slightly different way in each region but, if we introduce $\sigma = X^2 - T^2$, we see that

$$r = \frac{2M}{1 - \sigma/16M^2} \quad (\text{A6})$$

everywhere on the surface. Since $X^2 - T^2 < 16M^2$ for every point on our surface, r is a smooth function of X and T . It follows that Y is also a smooth function of X and T and that our surface is smooth.

Maple codes which can be used to plot this surface with and without Schwarzschild coordinate lines were given in sections III and IV respectively. The numerical integral in these codes is just equation (A5), though it takes a somewhat different form as it has been written using $q = \sigma/16M^2$ instead of r as the integration variable.

APPENDIX B: EMBEDDING OTHER SURFACES

In this appendix, we consider the embedding of other surfaces in 2+1 Minkowski space. Section B 1 shows that the radial plane of ‘normal’ static spherically symmetric star-like spacetimes can be so embedded. Thus, diagrams like fig. 7 can be generated for a large class of interesting spacetimes. On the other hand, section B 2 returns to the Kruskal spacetime, but considers a different totally geodesic surface, in this case one associated with observers who orbit the black hole but always remain inside the horizon. The pedagogical use of this latter embedding diagram is limited, but it does illustrate the crushing gravitational tidal ‘force’ of the black hole in the angular directions.

1. The radial planes of star-like objects

The metric for a general static spherically symmetric spacetime (without horizons) can be written in the form [12]

$$ds^2 = -e^{2\Phi} dt^2 + \frac{dr^2}{1 - 2m(r)/r} + r^2 d\Omega^2, \quad (B1)$$

where $m(r) = \int_0^r 4\pi r^2 \rho dr$ is the total mass-energy contained inside the radius r and the potential Φ satisfies

$$\frac{d\Phi}{dr} = \frac{m + 4\pi r^3 p}{r(r - 2m)}. \quad (B2)$$

Here, ρ is the energy density, p is the pressure, and we have set $c = G = 1$. For a static ‘normal’ star without horizons (or incipient horizons), we expect p , ρ , and $(1 - 2m/r)^{-1}$ to be bounded. Under these conditions, and assuming asymptotic flatness, the quantity $e^\Phi \left(\frac{d\Phi}{dr} \right) \sqrt{1 - 2m/r}$ is bounded, say by Q . We may then embed the radial plane of any such metric in region I of 2+1 Minkowski space by setting $\phi = Qt$ and following the same procedure used in section II. The function $Y(r)$ is determined by the equation

$$dY/dr = \sqrt{\frac{1}{1 - 2m/r} - e^{2\Phi} \left(\frac{d\Phi}{dr} \right)^2 Q^{-2}}, \quad (B3)$$

and, given the bound above, the square root is real. The resulting embedding diagram may be drawn by evaluating Φ , setting $\rho = e^\Phi/Q$ (and $s = \rho/4M$), and adjusting the definition of $Y1$ in the Maple code used for black hole region I in section IV to solve (B3), taking $Y1 = 0$ at some arbitrary radius r_0 .

2. The $r - \varphi$ plane of the Kruskal black hole

Another totally geodesic surface in the Kruskal spacetime is the analogue of fig. 1 inside the black hole. This is the surface given by $t = \text{const}$ and $\theta = \text{const}$ for $r < 2MG/c^2$, and its geometry is independent of either t or θ . All geodesics with zero momentum in the t, θ directions which start in this surface must remain there. Since we are considering the surface *inside* the black hole, this is again a timelike surface and we will wish to embed it in 2+1 Minkowski space. This can be done simply by taking r, φ to be the usual radius and polar angle in the XY plane and setting $r = 2M(1 - (\frac{T}{4M})^2)$. In fig. 21 below we have used a slightly different plotting scheme than in the main text for esthetic reasons.

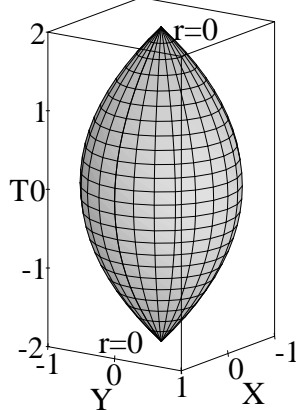


Fig. 21: The $t = \text{const}$, $\theta = \text{const}$ surface inside the Kruskal black hole, in units where $c = 1$ and $2MG/c^2 = 1$.

It is perhaps best to think of each circle above as representing a sphere of symmetry in the Kruskal geometry. Here we can see these spheres expanding through region III from zero size at the past singularity, reaching a maximum at $T = 0$ (the horizon, and in particular the bifurcation sphere – where regions I,II,III, and IV all meet), and then contracting again through region I back down to zero size. In this picture, the singularities appear at finite times $\frac{T}{2M} = \pm 2$ in the diagram and are clearly seen as corners at the top and bottom. However, we know that, in this surface also, the scalar curvature should diverge as we approach the singularity. This is not evident from the diagram and in fact (except for the corner at the singularity itself), the diagram looks rather flat in this region. What is happening is that the lines of constant θ in this surface are, once again moving at nearly the speed of light as seen from our reference frame ($dr/dT \rightarrow 1$ as $T \rightarrow 4M$). As a result, the diverging scalar curvature has once again been flattened out by an even more rapidly diverging boost.

On the other hand, the physical effects of the diverging curvature *are* quite clear. Consider, for example, a steel ring placed ‘around’ the black hole at $T = 0$. As time passes, if no part of this ring has any momentum in the directions transverse to the circle, the ring must simply move up the diagram. Because the entire diagram contracts to a point, the ring likewise must contract (i.e., be crushed) no matter how great a stress the ring can support⁶! This is one effect of the infinite crushing tidal gravitational ‘force’ in the direction around the black hole near the singularity.

⁶In ‘real life,’ of course, slight asymmetries would first cause the ring to buckle into the directions not shown on this diagram. In any case, the ring would be destroyed, no matter how strong it is.

REFERENCES

- [1] C. Misner, K. Thorne, and J. Wheeler, *Gravitation* (W.H. Freeman and Co., New York, 1971), pg. 837.
- [2] R. Geroch, *General Relativity from A to B*, (U. of Chicago Press, Chicago, 1978).
- [3] D. Mook and T. Vargish, *Inside Relativity*, (Princeton U. Press, Princeton, 1987).
- [4] W. Kauffman, *The cosmic frontiers of general relativity* (Little, Brown Pub., Boston, 1971).
- [5] R. Wald, *General Relativity*, (U. of Chicago Press, Chicago, 1984), pg. 148.
- [6] B. Berger, D.M. Chitre, V.E. Moncrief, and Y. Nutku, *Phys. Rev. D* **5** (1972) 2467; W. Unruh, *Phys. Rev. D* **14** (1972) 2467.
- [7] C. Callan, S. Giddings, J. Harvey, and A. Strominger, *Phys. Rev. D* **45** (1992) 1005, hep-th/9111056.
- [8] S. Giddings and A. Strominger, *Phys. Rev. D* **47** (1993) 2454, hep-th/9207034.
- [9] C. Misner, K. Thorne, and J. Wheeler, *Gravitation* (W.H. Freeman and Co., New York, 1971), e.g. pg. 826.
- [10] Ibid, pg. 834.
- [11] Ibid, pg. 820.
- [12] C. Misner, K. Thorne, and J. Wheeler, *Gravitation* (W.H. Freeman and Co., New York, 1971), pg. 604.

